Journal of Zhejiang University SCIENCE
ISSN 1009-3095
http://www.zju.edu.cn/jzus
E-mail: jzus@zju.edu.cn

Multidimensional modeling of Dimethyl Ether (DME) spray combustion in DI diesel engine*

WEN Hua (文 华)†, LIU Yong-chang (刘永长), WEI Ming-rui (魏明锐), ZHANG Yu-sheng (张煜盛)

(*School of Energy and Power Engineering, Huazhong University of Science and Technology, Wuhan 430074, China*)

†E-mail: d00wh@yahoo.com.cn

Received Nov. 4, 2003; revision accepted Feb. 12, 2004

Abstract: In the present study a modified CFD code KIVA3V was used to simulate the spray combustion in a small DI diesel engine fueled with DME. The improved spray models consider more spray phenomena such as cavitation flow in nozzle hole, jet atomization, droplet second breakup and spray wall interaction. Otherwise, a reduced DME reaction mechanism is implemented in the combustion model, and a new turbulent combustion model–Partial Stirred Reactor (PaSR) model is selected to simulate the spray combustion process, the effects of turbulent mixing on the reaction rate are considered. The results of engine modeling based on those models agreed well with the experimental measurements. Study of temperature fields variation and particle traces in the combustion chamber revealed that the engine combustion system originally used for diesel fuel must be optimized for DME.

Key words: Dimethyl ether (DME), Diesel engine, Spray combustion
doi:10.1631/jzus.2005.A0276 **Document code:** A **CLC number:** TK464

INTRODUCTION

The use of dimethyl ether (DME) as an alternative fuel appears to be a promising approach for simultaneously minimizing NO_x and soot emission from conventional diesel engines. The low self-ignition temperature of 508 K and the high oxygen content of 34.8 percent (mass fraction) are two major factors characterizing low soot and unburned total hydrocarbon (THC) emissions. Since the first introduction of the concept by Sorenson and Mikkelsen (1995), a number of studies (Fieisch *et al*., 1995; Kapus and Ofner, 1995; Zhou *et al*., 1999) suggested that DME might be widely used for diesel engines in trucks and buses where emission is a particular serious problem.

However, use of neat DME as a fuel for DI diesel engine leads to many problems, because the diesel engine was developed originally for diesel fuel rather than DME, whose physical and chemical properties are significantly different from those of diesel fuel. The formation of DME mixture gas in the diesel engine should be different from diesel, due to the easy evaporation of DME and mixing with air, and the auto-ignition and combustion are also different because of the higher cetane number of DME. Then, it is necessary to specially design the combustion system of engine for this fuel. Currently, multi-dimensional modeling has become an increasingly important tool for engine design and research. Using CFD model to simulate the process of DME spray combustion in the engine will be helpful for deep understanding of the working mechanism and for optimizing the combustion system for DME.

Although, there were many experiments on the use of DME in diesel engine, modeling research on DME spray combustion in diesel engine were mostly based on quasi-dimensional spray combustion model (Bek and Sorenson, 2001). One exception is the work of Golovitchev *et al*.(1998), who simulated two di-

* Project supported by the National Basic Research Program (973) of China (No. 2001CB209207) and the National Natural Science Foundation of China (No. 50376018)

mensional spray combustion in diesel engine after obtaining the new thermo-physical properties table and details of the DME reaction mechanism; but his model was only validated with experiments of DME spray combustion in constant volume chamber, not yet in diesel engine. For this reason, a three-dimensional modeling of the DME spray combustion in a diesel engine was implemented in this paper. Some modified sub-models such as spray model and combustion model were validated for DME spray combustion modeling after comparison showed that the computed results agreed well with the experimental results.

MODEL FORMULATION

The success of an engine CFD simulation depends on the modeling of the physical processes. The CFD code used in this paper is based on KIVA-3V (Amsden, 1997), which solves the conservation equations for evaporating fuel sprays coupled with three-dimensional turbulent fluid dynamics of compressible, multi-component, reactive gases in engine cylinders with arbitrarily shaped piston geometries. Some modifications in physical models had been incorporated into the code. The major model improvements in the spray and combustion models will be introduced here.

Spray model

Spray is a complicated physical phenomenon. The spray characteristics depend on fluid properties, ambient conditions, the fuel injector nozzle design specifications and operating conditions. Modeling spray is extremely important in injection engine combustion modeling.

1. Spray boundary

In this paper, the liquid injection is simulated using the 'blob' injection method of Reitz and Diwakar (1987). Boundary conditions of the liquid at the nozzle exit were obtained from a nozzle cavitation flow model (Wei *et al*., 2003). Nozzle cavitation processes dynamically influence the nozzle discharge coefficient and the effective nozzle exit area during the injection. This model calculates the instantaneous flow conditions inside the nozzle from the fuel mass flow rate, nozzle hole diameter and length, and inlet radius of curvature for rounded inlet nozzles. The effective exit velocity and area are calculated by applying corresponding continuity and momentum equations between the vena contracta and the nozzle exit.

2. Atomization and breakup model

The breakup of a liquid droplet moving in a gaseous environment is caused by the aerodynamic liquid-gas interactions (shear flow induced waves and drag-deceleration-induced waves). In this work, two mechanisms were used to characterize the breakup of the fuel droplets. The wave breakup model of Reitz and Diwakar (1987) considers the shearing-off of droplets due to the growth of Kevin-Helmholtz (KH) instabilities on the cylindrical liquid jet surface resulting from the relative velocity between the gas and liquid phases. Breakup due to the growth of Rayleigh-Taylor (RT) instabilities resulting from the deceleration of the injected droplet were also implemented. The concept of a breakup length to account for the dense spray region near the nozzle were used in conjunction with the KH and RT mechanisms (Ricart *et al*., 1997).

According to Reitz and Diwakar (1987), KH breakup model is governed by frequency of the fastest growing KH wave Ω_{KH}, and corresponding wavelength Λ_{KH}. During the breakup, the droplet radius reduces to stable radius r_c with uniform rate. In this case stable droplet radius r_c and breakup time τ_{KH} are given by

$$r_c = B_0 \Lambda_{KH} \tag{1}$$

$$\tau_{KH} = \frac{3.788 B_1 r}{\Omega_{KH} \Lambda_{KH}} \tag{2}$$

where B_0=0.61 and B_1 is constant parameter.

The rate of change of the droplet radius in the parcel due to droplet breakup is described using the following expression,

$$\frac{\mathrm{d}r}{\mathrm{d}t} = \frac{r - r_c}{\tau_{KH}} \tag{3}$$

Due to high initial velocities in the injected fuel, the liquid droplet decelerates rapidly with drag forces. Hence, RT instability may also play an important role on droplet breakup mechanisms in addition to the KH

instability. The equations for the wavelength Λ_{RT} and the frequency Ω_{RT} of the fastest growing RT wave are given as,

$$\Lambda_{RT} = 2\pi C_{RT} / K_{RT}$$
$$K_{RT} = \sqrt{\frac{-g_t(\rho_l - \rho_g)}{3\sigma}}$$
$$\Omega_{RT} = \sqrt{\frac{2}{3\sqrt{3\sigma}} \frac{[-g_t(\rho_l - \rho_g)]^{3/2}}{\rho_l + \rho_g}} \quad (4)$$

where g_t is the acceleration in the direction of droplet travel; C_{RT} is an adjustable constant.

In the present implementation of the RT model, the wavelength Λ_{RT} is compared to the droplet's diameter, and if the wavelength is small enough, RT waves are assumed to be growing on the surface of the droplet. The amount of time of wave growth is tracked and compared to the breakup time $\tau_{RH}=C_\tau/\Omega_{RT}$, where C_τ is RT breakup time constant. C_τ is determined to 9.0 within breakup length and 1.0 out of breakup length. If the disturbances grow long enough to become unstable, droplet occurs catastrophic breakup and immediately creates much smaller droplets. The diameter of the new droplets is assumed to be proportional to the RT wave Λ_{RT}.

The KH and the RT models compete in the jet breakup starting from the injector nozzle. Because two breakup mechanisms have different effect on droplet breakup within whole spray regions, the model has different constant on both sides of the breakup length. The liquid breakup length L_b under high injection pressure condition, is determined by

$$L_b = C_{bu} d_0 \sqrt{\rho_l / \rho_g} \quad (5)$$

where d_0 is the nozzle hole diameter; C_{bu} is model constant, and set equal to 10.0 in terms of Reitz and Diwakar (1987).

3. Spray and wall interaction model

Because the piston bowl in a small diesel engine is narrow, the DME spray impinging on the bowl wall is inevitable, especially under high load operation condition. The impact of a DME spray on the piston wall surface where temperature is usually beyond the boiling temperature of DME may lead to droplet breakup, to sudden vaporization, or to rebounding/splashing, or to development of a thin liquid film isolated by a thin vapor layer between fuel and wall. Among these, rebounding/splashing and film flow phenomena are considered in the current wall impingement sub-model (Amsden, 1997). In film flow model, the temperature of film surface adjacent to wall should not exceed the boiling temperature of DME, as a thin vapor layer is formed between them when the wall temperature exceeds the boiling temperature of DME.

Reaction mechanism

The combustion simulation based on a reduced but still detailed reaction mechanism which involving 27 species and 145 reactions was validated by simulating the auto-ignition of DME at constant pressure at various initial conditions (Golovitchev *et al*., 1998). It was implemented into the KIVA code in this work. Due to the stiffness of the chemical system formulation, a special technique, using a reference species (Amsden *et al*., 1989) for each reaction, was applied.

Combustion model

The Partially Stirred Reactor (PaSR) combustion model developed by Golovitchev (2000) was used to model the combustion process. This model is an extension of the Eddy Dissipation Concept (EDC) combustion model that is capable of using a more detailed chemistry mechanism, but the Eddy Dissipation Model (EDM) in the original KIVA3V code could not do it easily. Because detailed chemistry kinetic reaction is considered in this combustion model, there is no difference between auto-ignition and combustion model, it is no necessary to model the auto-ignition process again.

In the PaSR approach, a computational cell is split into two different zones, reaction zone and no reaction zone (Fig.1). The reaction zone is treated as a perfectly stirred reactor (PSR), in which all compositions is assumed to be perfectly mixed with each other. This allows us to disregard any fluctuations when calculating the chemical source terms. Three average concentrations are presented in the reactor, the mean mixture concentration of the feed c^0, the mixture concentration in the reaction zone c, the mixture concentration at the exit of the reactor c^1.

The whole combustion process could be regarded as two processes. The first is the initial

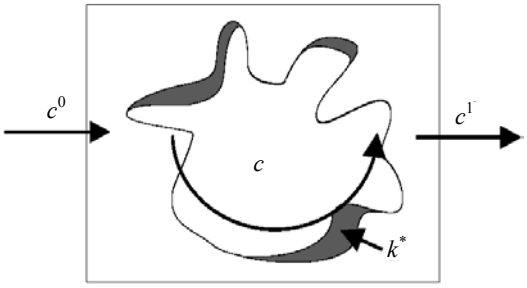

Fig.1 Conceptual diagram of PaSR Reactor (The reaction zone is painted)

concentration in the reaction zone changes from c^0 to c as it reacts; the second is the reaction mixture c is mixed with the no reaction mixture c^0 by turbulence, that results in the averaged concentration c^1. The reaction rate of this computational cell is determined by the fraction of the reactor in this cell. It seems quite clear that it should be proportional to the ratio of the chemical reaction time τ_{ch} to the total conversion time in the reactor, i.e. the sum of the micro-mixing time τ_{mix} and reaction time τ_{ch},

$$k^* = \frac{\tau_{ch}}{\tau_{mix} + \tau_{ch}} \tag{6}$$

The micro-mixing time τ_{mix} characterizes the exchange process between reaction mixture and no reaction mixture. In this paper micro-mixing time was obtained from the k-ε equation, $\tau_{mix}=c_{mix}k/\varepsilon$, the model constant c_{mix} was set to 0.015. This constant can, however, vary between 0.001–0.3, depending on the flow condition. The reaction time was derived from the laminar reaction rate. Thus, the overall reaction rate $\bar{\dot{\omega}}$ and the homogeneous reaction rate $\dot{\omega}$ of this computational cell have the following relationship,

$$\frac{c^1 - c^0}{\mathrm{d}t} = \bar{\dot{\omega}} = k^* \dot{\omega} \tag{7}$$

If τ_{mix} equals to zero, the whole cell is perfectly stirred. The combustion model reduced to the quasi-laminar combustion. If τ_{mix} dominates, the reaction rate is equivalent to the Magnussen-Hjertager eddy break-up rate. Then, the overall reaction rate in the PaSR model could be also regarded as the harmonic average of the quasi-homogeneous rate and the turbulent mixing control rate.

Initial conditions

The KIVA computations start from intake valve closure, then, a 1-D cycle simulation code (Wen *et al*., 2003) is used to provide the initial conditions, such as cylinder pressure, temperature and species fraction. The cycle simulation code considers the unsteady 1-D gas dynamics in the entire engine system geometry and is able to predict the gas exchange process and EGR levels. Thus, the effects of residual gas on the combustion of the subsequent cycle can be accounted for. The cycle simulation starts with fresh air and is executed for several engine cycles until the predicted cylinder pressure approached a steady state value.

ENGINE MODELING

The computational model developed was applied to ZS195 diesel engine (Table 1) fueled with DME. Some parameters of fuel supply system were adjusted, such as, the opening injection pressure being decreased from 18 MPa to 16 MPa, fuel delivery advance angle being increased to 26 °CA BTDC, and the diameter of plunger and nozzle hole being enlarged to 8.5 mm and 0.42 mm respectively.

Table 1 Engine and injection system specifications

Engine type	Changtong ZS195
Bore×stroke	95.0×115.0 mm
Connect rod length	210.0 mm
Compression ratio	17.5
Injection system	Pump-line-injector
Spray pattern	4 solid cones
Nozzle hole diameter	0.42 mm
Nozzle opening pressure	16.0 MPa

In the actual combustion chamber, the piston bowl has a little offset respect to the cylinder axis and four-hole injector. In order to limit the computational time, the 3D modeling of the spray combustion system simplifies the cylinder geometry as a symmetric. Then, a 90-degree sector of combustion chamber with a single nozzle are modeled, the computational mesh used in the present simulation is shown in Fig.2.

The modeling engine operational condition is that injection starts at −5 °CA ATDC with a duration time of 15 °CA (crank angle), injected mass is 55.08

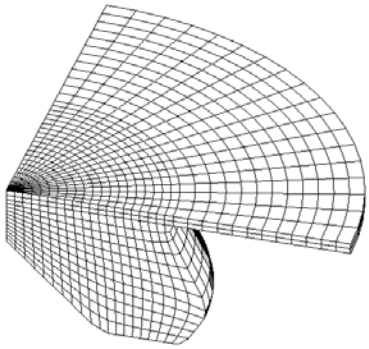

Fig.2 Computational mesh for ZS195 Engine

mg/cycle, injection rate shape specification is calculated according to the measured injection pressure at nozzle and initial swirl ratio of 1.8.

Before engine modeling, some spray breakup model adjustable constants should be determined by experimental result of spray characteristics; however, it is difficult to obtain the spray data in the actual combustion chamber. In this paper, spray liquid-phase length was computed by Siebers (1999)' analytic method, which is based on mixing limited vaporization and considers the conversation of mass, momentum and energy, was used to approximately scale those constants. Fig.3 presents the computed spray liquid and vapor penetration under different high ambient temperature condition in constant volume chamber with injector of ZS195. When the breakup model adjustable constant B_1 was set to 10, and C_{RT} was 0.1, 3D spray modeling showed satisfied results compared with those of analytic method. The penetration under different ambient temperature showed that the ambient temperature did not significantly influence the vapor penetration as observed in Siebers' experiment.

The final results of engine modeling are shown in Figs.4–5 by using the scaled breakup model constant. Fig.4 shows good agreement between computed and measured cylinder pressure and heat release rate data. The measured heat release rate data were obtained by applying a zero-dimensional model to the measured pressure data. It was found that the proportion of premix combustion was small compared with that of the traditional diesel engine, so the early heat release rate was low, and cylinder pressure increase rate was also low, corresponding to the small noise in DME engine operational experiments. The experimental results showed that at the end of the combustion process, an additional heat release was induced by the abnormal second injections due to the large pressure fluctuations in the injection line with DME, but it is not considered in the present model calculation. The combustion process is well predicted by the present model, which accounts for the effects of turbulent mixing and slow chemical reaction. It was also found that the accurate prediction of the ignition timing mainly relies on a reliable spray model and accurate model of the chemical reaction mechanism.

More detailed in-cylinder temperature contours and droplets distribution in a sequence of crank angles during spray and combustion are plotted in Fig.5, where two cross sections along the spray axis in vertical directions are shown. Fig.5 shows that the ignition delay time of DME is about 3 °CA, shortened as expected. The initial ignition spots and spray combustion zone in the combustion chamber appear close to the injector nozzle. Relatively strong spray wall

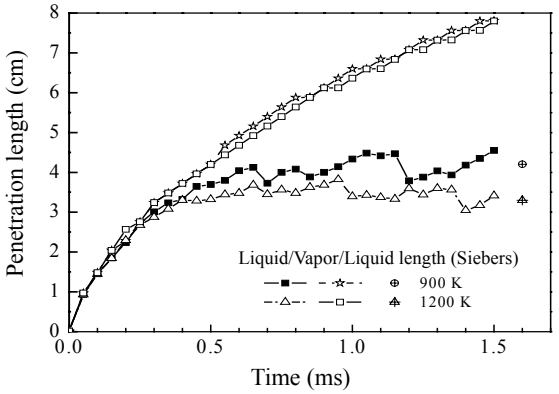

Fig.3 Penetration of the liquid and vapor phases at different ambient temperatures condition (ambient density of 15 kg/m^3)

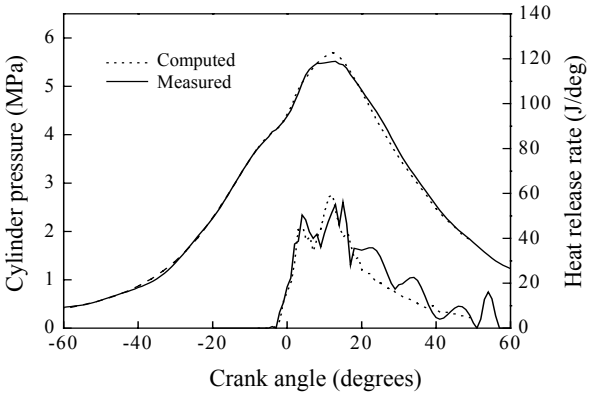

Fig.4 Comparison between computed and measured cylinder pressure and heat release rate

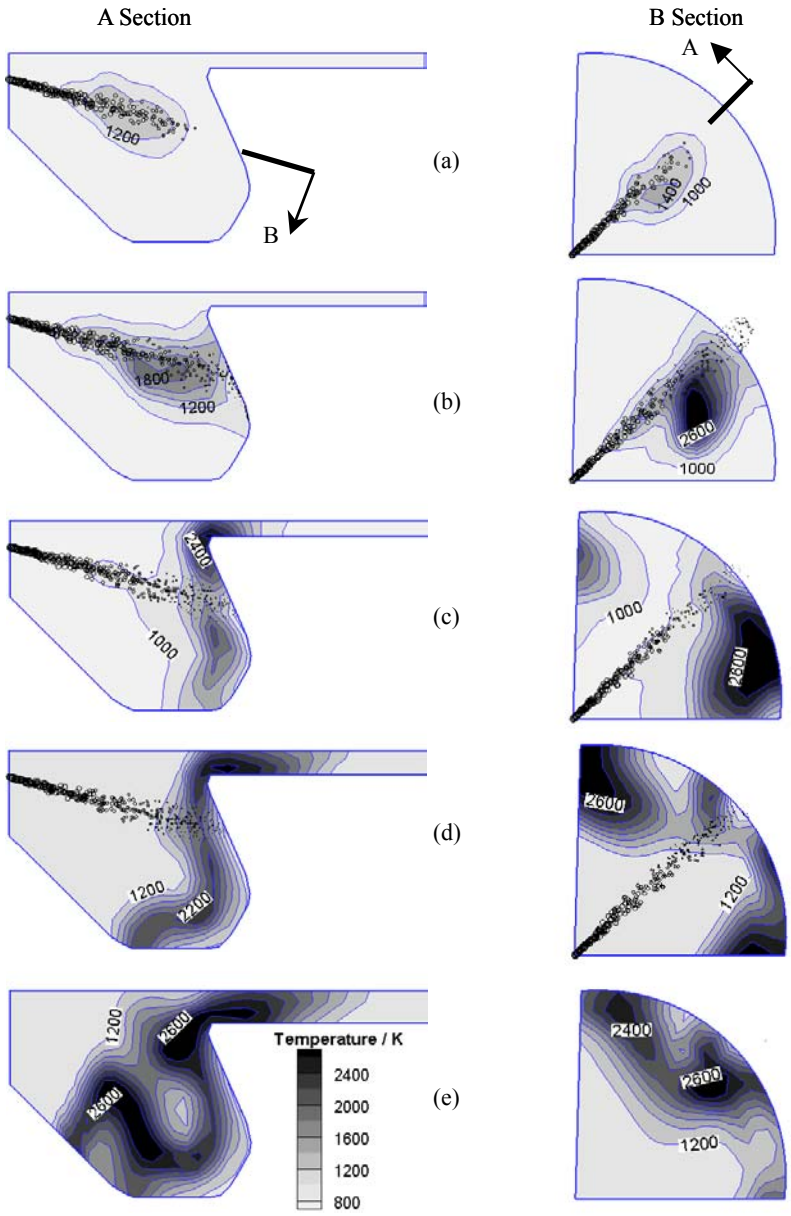

Fig.5 In-cylinder temperature and droplets distributions in a sequence of crank angles
(a) –2 °CA ATDC; (b) 0 °CA ATDC; (c) 4 °CA ATDC; (d) 10 °CA ATDC; (e) 20 °CA ATDC

impingement is observed at early combustion phase, as shown in Fig.5b. With the gas temperature increasing, the spray liquid length contracts, and spray wall impingement hardly occurs. Due to bowl swirl pushing the spray downward, the combustion zone transfers to the downstream of the swirl. In Fig.5d, it can be seen that the swirl has pushed the primary reaction zone to the adjacent spray and overlap with each other before the injection is over, which will lead to deteriorate the combustion. The main reason for the overlapping is the strong swirl and rapid fuel evaporation.

The biggest problem with DME used as a fuel is its high vapor pressure, low viscosity, and low heating value. These properties of DME result in too rapid fuel evaporation and early ignition. Then, it is necessary to improve the DME injection engine performance by optimizing the combustion system, in-

cluding its intake port, combustion chamber and injection rate shape specification.

Otherwise, no essential differences could be found between diesel and DME spray combustion. The combustion flame temperature of DME spray being not less than diesel's means the NO_x emission would not be significantly decreased compared with diesel. A better DME combustion mode such as homogeneous charge compression ignition (HCCI) mode, should be further investigated.

CONCLUSION

Development and validation of an integrated computer model for DME spray combustion is summarized in this paper. Those models have been used in engine modeling, where computed cylinder pressures and heat release rates agreed well with experimental measurements. Auto-ignition and combustion were predicted correctly using a detailed chemical kinetics mechanism, after proper scaling of the spray model constants. Simulation results are helpful for understanding the difference between diesel and DME spray combustion in diesel engine. Future research could apply CFD method as a useful tool for optimizing the combustion system of diesel engine for DME.

References

Amsden, A.A., O'Rourke, P.J., Butler, T.D., 1989. The KIVA-II: A Computer Program for Chemically Reactive Flows with Sprays. Los Alamos National Laboratory, Report No. LA-11560-MS.

Amsden, A.A., 1997. KIVA-3V: A Block-structured KIVA Program for Engine with Vertical or Canted Valves. Los Alamos National Laboratory, Report No. LA-13313-MS.

Bek, B.H., Sorenson, S.C., 2001. A mixing based model for dimethyl ether combustion in diesel engines. *Journal of Engineering for Gas Turbines and Power*, **123**(2):627-631.

Fieisch, T., McCarthy, C., Basu, A., 1995. A New Clean Diesel Technology: Demonstration of ULEV Emissions on A Navistar Diesel Engine Fueled with Dimethyl Ether. SAE Paper 950061.

Golovitchev, V.I., Nordin, N., Chomiak, J., 1998. Neat Dimethyl Ether: Is It Really Diesel Fuel of Promise? SAE Paper 982537.

Golovitchev, V.I., 2000. Revising Old Good Models: Magnussen Eddy Dissipation Concept. Proceedings of Topical Meeting on Modeling of Combustion, Turku, Finnland.

Kapus, P., Ofner, H., 1995. ULEV Potential of A DI/TCI Diesel Passenger Car Engine Operated on Dimethyl Ether. SAE Paper 952754.

Reitz, R.D., Diwakar, R., 1987. Structure of High Pressure Fuel Sprays. SAE Paper 870598.

Ricart, L.M., Xin, J., Bower, G.E., Reitz, R.D., 1997. In-cylinder Measurement and Modeling of Liquid Fuel Spray Penetration in A Heavy-duty Diesel Engine. SAE Paper 971591.

Siebers, D.L., 1999. Scaling Liquid-phase Fuel Penetration in Diesel Sprays Based on Mixing-limited Vaporization. SAE Paper 1999-01-0528.

Sorenson, S.C., Mikkelsen, S.E., 1995. Performance and Emissions of A 0.273 Liter Direct Injection Diesel Engine Fueled with Neat Dimethyl Ether. SAE Paper 950964.

Wei, M.R., Liu, Y.C., Wen, H., Zhang, Y.S., 2003. The orifice flow model and its effect on the calculations of high pressure sprays. *Transaction of CSICE*, **21**(4):228-233 (in Chinese).

Wen, H., Liu, Y.C., Wei, M.R., 2003. 1-Dimensional unsteady flow simulation of internal combustion engine intake and exhaust system based on space-time conservation method. *Small Internal Combustion Engine and Motorcycle*, **32**(1):29-31(in Chinese).

Zhou, L.B., Wang, H.W., Jiang D.M., Huang, Z.H., 1999. Study on Performances and Combustion Characteristics of DME Fueled Light Duty Direct-injection Diesel Engine. SAE Paper1999-01-3669.